



Since January 2020 Elsevier has created a COVID-19 resource centre with free information in English and Mandarin on the novel coronavirus COVID-19. The COVID-19 resource centre is hosted on Elsevier Connect, the company's public news and information website.

Elsevier hereby grants permission to make all its COVID-19-related research that is available on the COVID-19 resource centre - including this research content - immediately available in PubMed Central and other publicly funded repositories, such as the WHO COVID database with rights for unrestricted research re-use and analyses in any form or by any means with acknowledgement of the original source. These permissions are granted for free by Elsevier for as long as the COVID-19 resource centre remains active.



Qualitative and quantitative DECT pulmonary angiography in COVID-19 pneumonia and pulmonary embolism



C.D. Arru^{a,c}, S.R. Digumarthy^{a,*}, J.V. Hansen^b, M.D. Lyhne^b, R. Singh^a,
R. Rosovsky^a, J.E. Nielsen-Kudsk^b, C. Kabrhel^a, L. Saba^c, M.K. Kalra^a

^a Massachusetts General Hospital, 55 Fruit Street, Boston, MA, USA

^b Department of Cardiology, Department of Clinical Medicine, Aarhus University Hospital, Palle Juul Jensens Boulevard 99, 8200 Aarhus N, Denmark

^c Azienda Ospedaliera Universitaria, SS 554 km 4,500, Monserrato, 09042, Cagliari, Italy

ARTICLE INFORMATION

Article history:

Received 22 September 2020

Accepted 17 February 2021

AIM: To assess differences in qualitative and quantitative parameters of pulmonary perfusion from dual-energy computed tomography (CT) pulmonary angiography (DECT-PA) in patients with COVID-19 pneumonia with and without pulmonary embolism (PE).

MATERIALS AND METHODS: This retrospective institutional review board-approved study included 74 patients (mean age 61 ± 18 years, male:female 34:40) with COVID-19 pneumonia in two countries (one with 68 patients, and the other with six patients) who underwent DECT-PA on either dual-source (DS) or single-source (SS) multidetector CT machines. Images from DS-DECT-PA were processed to obtain virtual mono-energetic 40 keV (Mono40), material decomposition iodine (MDI) images and quantitative perfusion statistics (QPS). Two thoracic radiologists determined CT severity scores based on type and extent of pulmonary opacities, assessed presence of PE, and pulmonary parenchymal perfusion on MDI images. The QPS were calculated from the CT Lung Isolation prototype (Siemens). The correlated clinical outcomes included duration of hospital stay, intubation, SpO₂ and death. The significance of association was determined by receiver operating characteristics and analysis of variance.

RESULTS: One-fifth (20.2%, 15/74 patients) had pulmonary arterial filling defects; most filling defects were occlusive (28/44) located in the segmental and sub-segmental arteries. The parenchymal opacities were more extensive and denser (CT severity score 24 ± 4) in patients with arterial filling defects than without filling defects (20 ± 8 ; $p=0.028$). Ground-glass opacities demonstrated increased iodine distribution; mixed and consolidative opacities had reduced iodine on DS-DECT-PA but increased or heterogeneous iodine content on SS-DECT-PA. QPS were significantly lower in patients with low SpO₂ ($p=0.003$), intubation ($p=0.006$), and pulmonary arterial filling defects ($p=0.007$).

CONCLUSION: DECT-PA QPS correlated with clinical outcomes in COVID-19 patients.

© 2021 The Royal College of Radiologists. Published by Elsevier Ltd. All rights reserved.

DOI of original article: <https://doi.org/10.1016/j.crad.2021.02.008>.

* Guarantor and correspondent: S. R. Digumarthy, Massachusetts General Hospital, 55 Fruit Street, Boston, MA, USA. Tel.: +617 724 2275.
E-mail address: sdigumarthy@mgh.harvard.edu (S.R. Digumarthy).

<https://doi.org/10.1016/j.crad.2021.02.009>

0009-9260/© 2021 The Royal College of Radiologists. Published by Elsevier Ltd. All rights reserved.

Introduction

Patients with coronavirus 2019 (COVID-19) infection are reported to have endothelial dysfunction, activation of coagulation, thromboembolic disease, and disseminated intravascular coagulation.^{1–3} Vascular complications, such as deep vein thrombosis, pulmonary thromboembolism, systemic arterial thrombi and emboli, myocardial ischaemia, and ischaemic stroke, are reported in patients with COVID-19 infection.^{3–7} Occlusions in the pulmonary arterial circulation are thought to be related to severe disease and higher mortality in COVID-19 infection,⁸ although the exact causes for disease severity and host response remain unclear.

It is also unclear if patients with COVID-19 pneumonia develop PE or in situ thrombi, and if imaging can differentiate between these two entities. Peripheral venous thrombosis was absent in most COVID-19 patients but these patients were diagnosed with PE,³ raising the possibility of in situ thrombi in the pulmonary arterial circulation. Although prophylaxis and treatment of PE in patients with COVID-19 pneumonia is of increasing clinical interest, it is unclear if pulmonary arterial in situ thrombosis should be treated in a similar fashion to PE.^{3,9}

To be detectable on computed tomography (CT), pulmonary arterial filling defects must extend beyond the pulmonary microcirculation to at least segmental or proximal subsegmental pulmonary arteries or lead to assessable changes in pulmonary perfusion.¹⁰ Quantitative lung parenchymal perfusion (QPS) has been assessed in non-COVID-19 patients with PE using DECT pulmonary angiography (DECT-PA) perfusion maps and material decomposition iodine (MDI) images.¹¹ Recent publications in COVID-19 patients have described decreased perfusion in consolidative opacities surrounded by a “hyperaemic halo” of increased perfusion and dilated adjacent pulmonary arteries on DECT^{12,13} without a clear explanation for these findings. There is increasing evidence that DECT-PA can depict changes in pulmonary perfusion in the absence of visible PE and in situ thrombi.^{14,15} The present study assessed differences in qualitative and quantitative pulmonary perfusion from DECT-PA in patients with COVID-19 pneumonia with and without visible filling defects in the pulmonary arteries.

Materials and methods

Patients and protocols

The institutional review boards approved this retrospective study with a waiver of informed consent at both Massachusetts General Hospital (Site A) and Aarhus University Hospital (Site B). This retrospective study included 74 adult patients with reverse transcription polymerase chain reaction (RT-PCR) confirmed COVID-19 pneumonia from two quaternary hospitals (site A: 68 patients, site B: six patients). All patients underwent DECT-PA for suspected PE as part of clinical care.

Details were recorded regarding duration of hospital stay (<10 days or \geq 10 days), disease outcome (death or discharge with recovery), intubation status (yes or no) and peripheral oxygen saturation (SpO₂; low <90%; normal \geq 90%) at the time of DECT-PA. No patients were excluded based on their size or body mass index.

Patients from site A underwent DECT-PA on either a dual-source (DS), 192-section multidetector-row CT machine (Siemens Definition Force, Siemens Healthineers; $n=45$ patients) or single-source (SS), 64-slice multidetector-row CT (GE Discovery 750HD, GE Healthcare; $n=23$ patients). The imaging parameters for DS-DECT-PA were 80/150 kV with tin filter, automatic exposure control (CareDose 4D, Siemens Healthineers) at quality reference tube current of 180 mAs, 1.1:1 pitch, 0.28-second gantry rotation time, and 192 \times 0.6 detector configuration. The SS-DECT-PA examinations were performed at 80/140 kV with rapid voltage-switching, fixed tube current of 280–360 mA, 0.5-second rotation time, 1.375:1 pitch, and 64 \times 0.625 detector configuration.

Site B patients were scanned on a dual-source, 128-section multidetector-row CT (Siemens Definition Flash; $n=6$ patients). The imaging parameters for DS-DECT-PA were 100/140 kV with tin filter, automatic exposure control (CareDose 4D) at quality reference tube current of 180 mAs, 1.1:1 pitch, 0.28-second gantry rotation time, and 128 \times 0.6 detector configuration.

All patients at both sites received 350–370 mg iodine/ml iodinated contrast media injected at 4–5 ml/second (80 ml for patients \leq 80 kg body weight; 100 ml for patients >80 kg body weight). Images were reconstructed at 1–1.25 thickness with 50% overlap. For all DECT-PA, transverse virtual mono-energetic (Mono 40 keV) and material decomposition iodine (MDI) images were generated.

Qualitative evaluation

Two thoracic radiologists (SRD and MKK with 16 and 13 years of experience) reviewed Mono 40 keV and MDI images in consensus to assess COVID-19 pneumonia-related lung findings, filling defects in pulmonary arteries, and qualitative perfusion abnormalities. As the DS-DECT-PA MDI images segment the inflated lungs and exclude the opacified lungs, the 40 keV images were reviewed to assess contrast enhancement within regions of opacities to differentiate pulmonary opacities related to pneumonia and pulmonary infarction. Imaging findings and severity were assessed on 40 keV images to score severity and type of opacities. Based on prior publications,^{16,17} the COVID-19 pneumonia-related findings were graded separately in each of the five lung lobes for extent (0, no pulmonary opacity; 1, opacities involving <5% lobar volume; 2, 5–25% lobar involvement; 3, 26–50% lobar involvement; 4, 51–75% lobar involvement; 5, >76% lobar involvement) and type of opacities (1, ground-glass opacities 2, consolidation or mixed opacities such as ground-glass opacities with consolidation, interlobular septal thickening or nodules). For each lobe, the extent and type of pulmonary opacities were added to obtain lobar involvement scores (maximum score of 5). The entire lung severity score was obtained by

adding lobar scores for all the five lobes (maximum score of 35). Also, contrast enhancement (from Mono 40 keV) and iodine uptake (from MDI) in regions of pulmonary opacities was recorded (as decreased, increased, or variable relative to the adjacent normal lung). Radiologists could adjust the window levels and widths at their discretion.

Both radiologists assessed pulmonary arterial filling defects for location (from main pulmonary trunk to subsegmental arteries) and degree of occlusion (occlusive, non-occlusive). The number (one score for each positive pulmonary arterial filling defect) of pulmonary arterial filling defects was recorded. The presence of focal or diffuse dilatation, narrowing, wall thickening, and irregularity of pulmonary arteries and veins was also recorded. The presence and type of opacities (normal lung parenchyma, ground-glass, consolidation, or mixed opacities) were assessed in the lung supplied by the pulmonary artery with filling defect. The presence and lobar location of pulmonary infarction were recorded. The radiologists also assessed for right heart strain (ratio of right to left ventricle diameters and flattening or leftward bowing of the interventricular septum), and the diameter of the main pulmonary trunk. A study co-investigator (C.A.) reviewed dictated radiology reports of included DECT-PA to record PE documentation.

Quantitative evaluation

The low and high voltage DS-DECT-PA were processed with the lung lobe segmentation and perfusion analysis software (CT Lung Isolation, eXamine, Siemens Healthineers, Forchheim, Germany). The artificial intelligence-based software automatically estimates quantitative perfusion statistics (QPS) from DS-CT over the entire volumes of both lungs, right lung, and left lung, as well as the five lung lobes (Fig 1).¹¹ QPS includes contrast media amount, concentration, mean and median contrast enhancement, standard deviation, variance, skewness, and kurtosis of iodine distribution in the entire lung and individual lung lobes. These QPS features are generated automatically by the software and cannot be individually verified by the users. An important distinction between the qualitative evaluation of perfusion and QPS was that for the former, both radiologists assessed lung perfusion in regions with and without parenchymal opacities, whereas QPS quantifies lung regions without dense parenchymal opacities (consolidation, infarcts, or atelectasis). DS-DECT-PA image series in two patients (2/51) could not be processed with the software. The software is designed for DS-DECT-PA, and therefore the SS-DECT-PA images were not assessed for QPS.

Statistical analyses

Data were analysed with Microsoft EXCEL (Microsoft, Redmond, WA, USA). Apart from the descriptive statistics, one-way analyses of variance (ANOVA) was performed to determine the differences in severity scores, pulmonary arterial filling defects, and QPS for patients with low and normal SpO₂, intubation (yes or no), hospital admission

duration (<10 days, ≥10 days), and outcomes (death versus recovery). For statistically significant parameters, receiver operating characteristics (ROC) curve analyses was performed to determine the area under the curve (AUC). A *p*-value of <0.05 was considered a statistically significant difference.

Results

Clinical features and outcomes

There were 74 adult patients with COVID-19 pneumonia (age range 21–96 years; mean age 61±18 years; 40 females and 34 males). At the time of DECT-PA, 54% (40/74) were on anticoagulants (heparin, warfarin, rivaroxaban, or enoxaparin) as part of their standard of care treatment, 45% were admitted for ≥10 days (33/74), 59% had SpO₂ of <90% (44/74), and 22% were intubated (16/74). The mortality rate in this group was 14% (10/74; Table 1).

Lung parenchymal assessment and severity scores

There were changes in the lung parenchyma in 97% of patients (72/74). Of these, 89% (64/72) had mixed parenchymal opacities comprising ground-glass and consolidation, and 11% (8/72) had pure ground-glass opacities. The regions with pure ground-glass opacities had increased perfusion compared to the adjacent normal lung parenchyma on the qualitative assessment of all MDI images (Figs 2–4); however, patients with mixed or consolidative opacities demonstrated a scanner-specific appearance of lung perfusion (Figs 2–4). The consolidative and mixed opacities demonstrated lower perfusion than normal lung parenchyma on the DSCT-PA MDI (Figs 2–4), but increased or heterogeneous perfusion on SS-DECT-PA MDI. There were no regions of hyper-perfusion in lung parenchyma adjacent to consolidative or mixed opacities in any patient. The CT severity score was lower in patients with pure ground glass (CT severity score 13±5) compared to patients with mixed and consolidative opacities (CT severity score 22±6). The CT severity scores independently did not predict the disease outcomes (death, mechanical ventilation, low SpO₂, or hospital stay duration: AUC<0.53, *p*>0.4). There was no significant difference in the CT severity scores between the SS-DECT-PA (20.1±6.7) and DS-DECT-PA (20.5±7.9; *p*=0.83).

Pulmonary vascular changes

Approximately 20% of patients had pulmonary arterial filling defects (15/74), and of these, 53% were on prophylactic anticoagulation (8/15). There were 53 pulmonary arterial filling defects with three in the main pulmonary arteries and the other 50 in lobar and distal branches. Most filling defects were in subsegmental or segmental branches (44/53; 83%) and mostly within the lower lobes (32/50; 64%; Table 2). Only one patient with extensive PE had evidence of right heart strain with the right to left ventricle ratio of 1.3 and straightening of the interventricular septum.

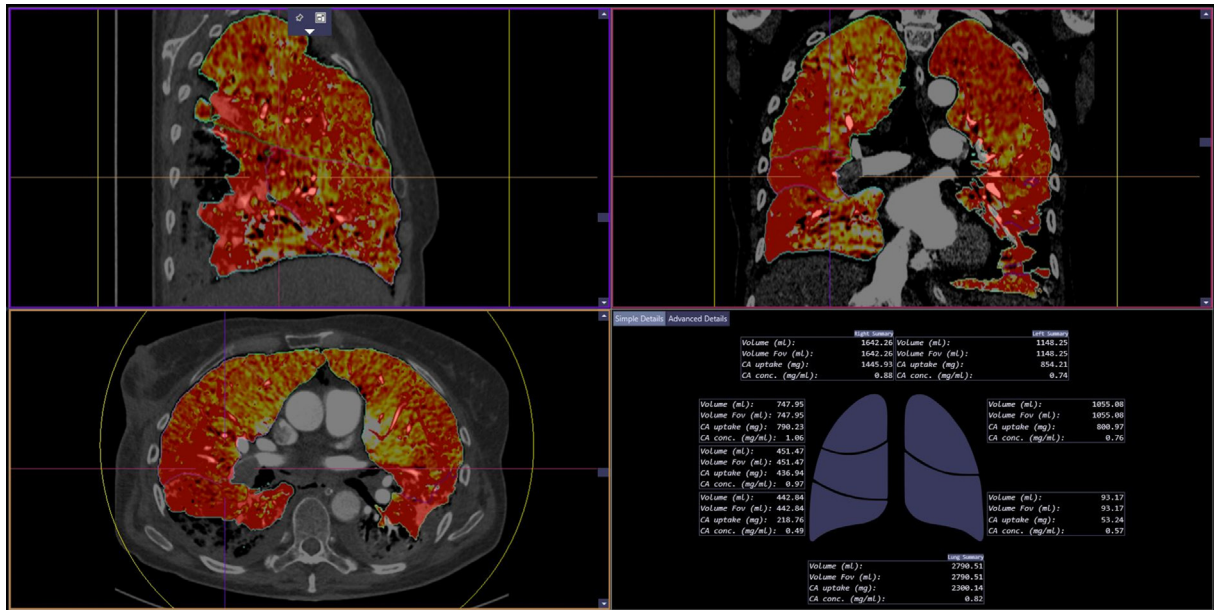


Figure 1 QPS software in action. The software automatically generates MDI images in the transverse, coronal and sagittal planes as well as a diagrammatic (bottom right image) and tabular representation (not shown) of QPS features for the whole lung, right lung, left lung, and each lung lobe.

The lung parenchyma adjacent to the arterial filling defects in the lungs had consolidative or mixed (ground-glass opacities with consolidation or interlobular septal thickening) opacities in 80% (12/15) and only ground-glass opacities in 20% (3/15) patients. Six patients (40%) had pulmonary infarcts and were associated with occlusive segmental or subsegmental filling defects in lower lobes. Infarcts were non-enhancing, pulmonary opacities with a broad pleural base on mono-energetic images and as regions of perfusion defects on MDI images (Fig 3). There were no PE in three patients (3/74) with deep venous thrombosis in the upper or lower extremities. None of the patients had pulmonary arterial wall thickening, irregularity, dilatation, beading, or aneurysm, and none had filling defects in cardiac chambers or systemic arteries. The severity scores for pulmonary involvement were higher in patients with pulmonary arterial filling defects (mean score 24 ± 4 compared to mean score 19 ± 8 ; $p=0.02$). The presence of pulmonary

arterial filling defects, however, did not affect any outcome measure.

QPS

The QPS (contrast agent amount, kurtosis, variance, 10th and 25th percentile values) were strong predictors for patient intubation (AUC 0.75–0.77; $p=0.0052$ –0.0012) and duration of hospital stay (AUC 0.83, 95% confidence interval 0.68–0.91; $p<0.0001$). The deceased patients and patients with low SpO₂ had significant differences in these QPS features compared to survivors and those with high SpO₂ ($p<0.05$; Table 3) but was also associated with AUC (<0.68) suggestive of significant overlap in perfusion statistics within the groups.

There were significant differences in QPS in patients with and without PE ($p=0.0045$ –0.0006) with the most important predictors being mean, modal, and 10th percentile of iodine-related contrast enhancement in Hounsfield units on MDI images (AUC 0.73–0.75). The mean and mode values were significantly lower in patients with PE ($p=0.0045$). There was no significant difference in any QPS features between patients on anticoagulation and without ($p>0.1$). As QPS assesses perfusion in the aerated portions of each lung and lobes and excludes regions with dense opacities, there was reduced iodine concentration and contrast enhancement in lung lobes with consolidative or mixed opacities that demonstrated decreased qualitative perfusion. Despite the qualitative differences in perfusion on MDI images, there was no difference in QPS features between GGO (iodine concentration 1.7 ± 0.7 mg/ml) and normal lung parenchyma (iodine concentration 1.4 ± 0.4 mg/ml; $p=0.73$).

Table 1
Summary of the clinical features and outcomes.

Patients	74 patients (68 from site A; 6 from site B)	
Gender	40 females, 34 males	
Age	61 \pm 18 years (average \pm standard deviation)	
	Yes	No
Prophylactic anticoagulation	40 (54%)	34 (46%)
Low SpO ₂	44 (59%)	30 (41%)
Intubation	16 (22%)	58 (78%)
Pulmonary embolism	15 (20%)	59 (80%)
Hospital stay	45 (61%)	29 (39%)
Death	10 (14%)	64 (86%)

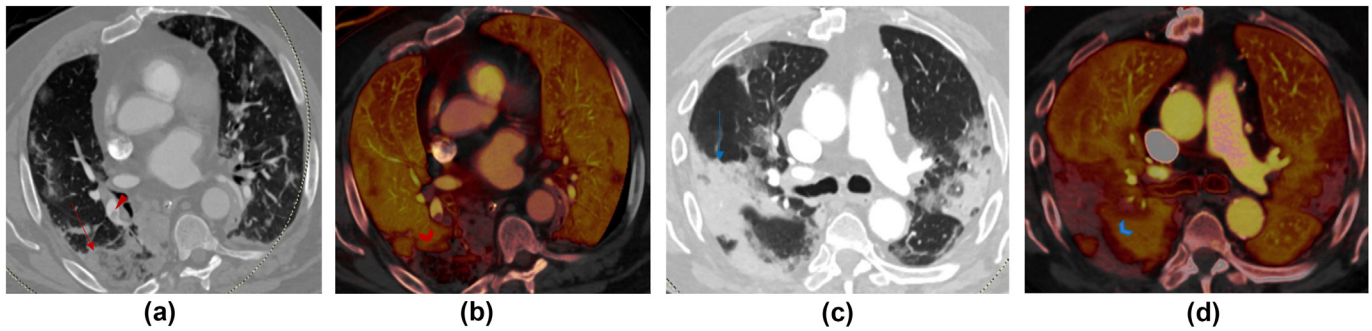


Figure 2 (a,c) Transverse virtual mono-energetic (Mono 40 keV) and (b,d) material decomposition iodine (MDI) images belonging to two patients scanned with DS-DECT-PA. (a) Mono 40 keV image of a 67-year-old COVID-19 infected man demonstrates a mixed ground-glass and consolidative opacity in the right lower lobe (red arrow) and pulmonary embolus in the segmental right lower lobe pulmonary arteries; (b) the MDI image demonstrates decreased lung perfusion in the region of the mixed opacity consistent with a pulmonary infarction. (c) Mono 40 keV image of an 80-year-old man has multifocal consolidations in bilateral upper and right lower lobes, which correspond to regions of perfusions defects on MDI image (d). Both patients had RT-PCR positive COVID-19 pneumonia.

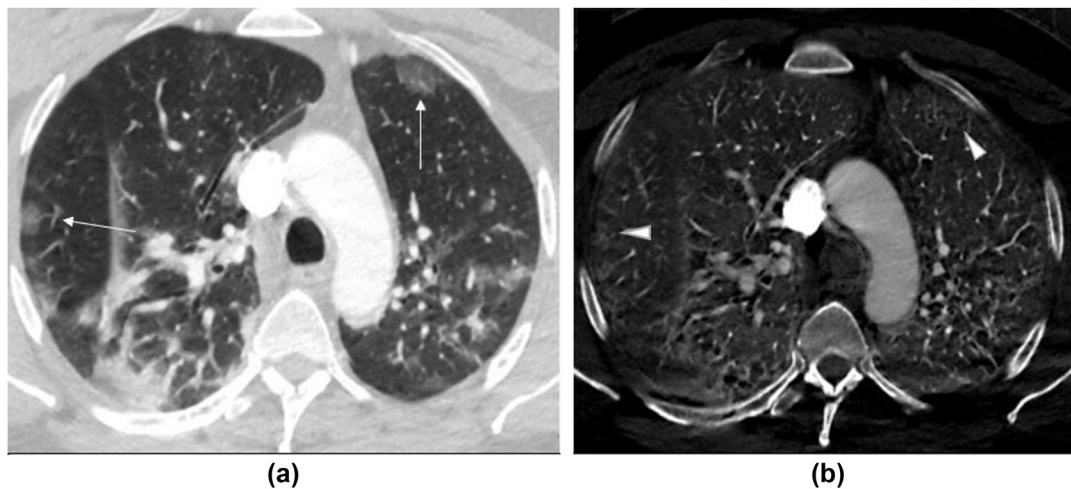


Figure 3 (a) Transverse virtual mono-energetic (Mono 40 keV) and (b) material decomposition iodine (MDI) images of a 48-year-old COVID-19 infected man with SS-DECT-PA. Mono 40 keV images demonstrate ground-glass opacities in bilateral upper lobes (along arrows), which correspond to regions of increased perfusion (iodine related enhancement) on MDI images. The consolidative opacity in the right lower lobe demonstrates variable perfusion pattern.

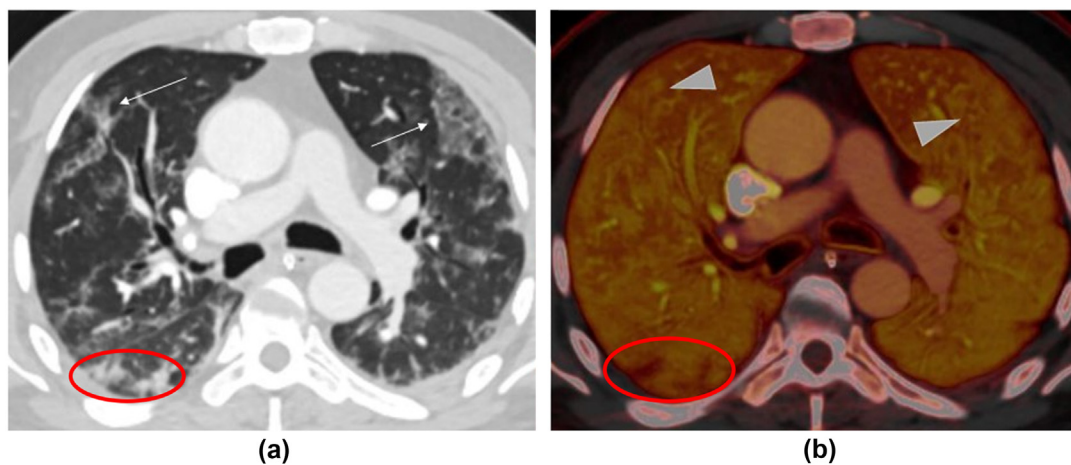


Figure 4 (a) Transverse virtual mono-energetic (Mono 40 keV) and (b) material decomposition iodine (MDI) images of a 54-year-old COVID-19 infected man who underwent DS-DECT-PA. Mono 40 keV images demonstrate ground-glass opacities in the bilateral upper lobes (along arrows), which correspond to regions of increased perfusion (arrowheads) on MDI images. The nodular foci of consolidation in the right lower lobe demonstrate decreased perfusion compared to the adjacent normal lung (within the red ovals).

Table 2
Summary of distribution of PE at different levels and lung lobes.

Location	Occlusive PE	Non-occlusive PE	Total PE
<i>Overall distribution</i>			
Main pulmonary trunk	0	0	0
Right and Left main PA	0	3	3
Lobar PA	0	6	6
Segmental PA	8	7	15
Subsegmental PA	20	9	29
<i>Lobar distribution</i>			
Right upper lobe PA	0	1	1
Right middle lobe PA	10	0	10
Right lower lobe PA	8	7	15
Left upper lobe PA	4	3	7
Left lower lobe PA	6	11	17

Most PE were in segmental and subsegmental arteries of the lower lobes. PE, pulmonary emboli; PA, pulmonary arteries.

There were significant differences ($p < 0.0001$) in QPS in patients with extensive versus non-extensive COVID-19 pneumonia based on the severity scores (AUC of up to 0.83; 95% confidence interval 0.69–0.91) with best predictors being 10th and 25th percentile of iodine-related contrast enhancement, kurtosis, and contrast agent concentration from the MDI images (lower in patients with extensive disease as compared to those with a non-extensive disease). This was true both on the entire lung severity scores (combined scores for all lung lobes) and lobe-specific severity scores (AUC 0.82–0.86, $p < 0.0001$).

Discussion

There is a significant difference in QPS of the lung in COVID-19 patients for outcomes such as duration of hospital stay, need for intubation, low SpO₂, and mortality. There is a high prevalence of pulmonary arterial filling defects in

patients with higher CT severity scores. Still, pulmonary arterial filling defects did not affect the clinical outcome and are not associated with peripheral vein thrombosis. The qualitative perfusion changes noted on mono-energetic and material decomposition images of DECT are scanner specific and vary with a SS-DECT and DS-DECT scanners.

DECT allows estimation of iodine concentration in each image voxel and therefore, can assess the distribution of intravenously injected iodinated contrast medium in the lung parenchyma and lung perfusion. The derived QPS are based on deep learning algorithms and have been shown to represent quantitative lobar perfusion accurately in patients with pulmonary embolism.¹¹ In the present study, QPS correlated to outcomes such as duration of hospital stay, need for intubation, low SpO₂, and mortality and was independent of the presence of pulmonary embolism and CT severity score. These results suggest that there are perhaps changes in the microcirculation that affect the perfusion of the lung. The changes in the microcirculation may be related changes induced by parenchymal opacities and ventilation. These changes may be secondary to hypoxia-related vasoconstriction or direct involvement of the vessels. Autopsy and pathology studies have demonstrated endothelitis in COVID-19 pneumonia that resulted in multiorgan failure and ischaemia in the kidney and small intestine.² These findings support observations that decreased QPS was noticed in patients without pulmonary arterial filling defects and was associated with severe diseases such as consolidation and mixed opacities.

Lower kurtosis was noted in patients with adverse outcomes (disease survival, shorter hospital admission duration, and normal SpO₂) as opposed to those with favourable outcomes. Lower kurtosis implies lower probability of extreme values and a wider spread of values around the mean of distribution. With more severe disease, such as with cor pulmonale or increased pulmonary vascular

Table 3
Summary of disease outcome variables and quantitative perfusion statistics (QPS) that demonstrated significant statistical differences ($p < 0.05$).

Outcome variables	No. patients	Contrast agent (amount in mg)	Kurtosis	Total lung volume (ml)	Variance of CT values (HU)	10 th percentile	25 th percentile	CT severity score
Disease outcome								
Survived	46 (S) 18 (GE)	4,176 ± 1,440	13.8 ± 12.1	2,864 ± 1,001	1,351 ± 939	-0.81 ± 12.7	17.5 ± 12	20 ± 8.2
Deceased	6 (S) 4 (GE)	3,829 ± 1,671	7.9 ± 3.8	2,381 ± 863	1,295 ± 430	3.6 ± 6.7	22 ± 12	22 ± 9.2
Hospital stay duration								
≥10 days	33 (S) 12 (GE)	3,902 ± 1,283	11.5 ± 10.8	2,731 ± 981	1,596 ± 1,021	-3.9 ± 14	14.3 ± 12.4	20.6 ± 7.8
<10 days	18 (S) 11 (GE)	4,481 ± 1,664	15.8 ± 12.6	2,953 ± 990	966 ± 412	4.5 ± 5.7	23.3 ± 9.6	20.1 ± 9.3
Intubation + mechanical ventilation								
Present	11 (S) 5 (GE)	4,414 ± 1,798	15.3 ± 15.9	2,921 ± 849	2,108 ± 1,422	-9 ± 15.5	10 ± 10.4	21.7 ± 8.6
Absent	40 (S) 18 (GE)	4,037 ± 1,358	12.5 ± 10.3	2,786 ± 1,019	1,174 ± 597	1.3 ± 11	19.6 ± 11.9	20.1 ± 8.3
SpO ₂								
Normal (>95%)	25 (S) 5 (GE)	4,335 ± 1,502	13.4 ± 10.1	2,903 ± 980	1,188 ± 579	1.8 ± 9.2	19.6 ± 11.4	18.5 ± 9.8
Reduced	26 (S) 18 (GE)	3,902 ± 1,386	12.8 ± 13	2,727 ± 992	1,534 ± 1,108	-3.3 ± 14.9	15.8 ± 12.8	22.3 ± 6.2

S, Siemens; GE, General Electric.

resistance, there is greater lung involvement with denser opacities (consolidation) and fewer regions with normal lung parenchyma. These findings in turn decrease the probability of extreme attenuation and iodine values, which was likely responsible for a smaller kurtosis value in patients with adverse outcomes. A recent study reported that pulmonary perfusion defects on DECT-PA were not related to increased pulmonary vascular resistance or cor pulmonale.¹⁵

Like DS-DECT-PA MDI images, the QPS software segments the inflated, non-opacified portion of the lungs and quantifies iodine distribution in those portions only. Thus, any portion of the lungs with dense pulmonary opacities, such as from consolidation, atelectasis, and pulmonary infarctions, are excluded from estimation of QPS features. The QPS software will therefore show decreased iodine distribution in the presence of ischaemic loss of perfusion (from pulmonary emboli, perfusion defects with and without pulmonary infarction) and from exclusion of opacified pulmonary parenchyma from any non-ischaemic process (Fig 5). In both instances, the overall estimated lung perfusion from QPS will decrease, and therefore, QPS can be used for quantifying the effect of disease burden in absence of true pulmonary perfusion defects of ischaemic aetiology.

In the present study, 20% of patients (15/74) with COVID-19 infection that underwent DECT-PA had pulmonary arterial filling defects. More than half were receiving prophylactic anticoagulation at the time of diagnosis, and none had documented DVT. In three patients with documented peripheral DVT, no PE was detected. These findings concur with Poissy *et al.*¹⁸ who reported pulmonary emboli in >20% of COVID-19 patients with a median intensive care unit (ICU) stay of 6 days. The overwhelming majority of 91% in their study were also receiving prophylactic anticoagulation, and the incidence of DVT was only 4.7%.

Therefore, it is not clear if the filling defects in pulmonary arteries truly represent emboli originating from thrombus elsewhere or represent in situ thrombi in pulmonary arteries. No specific features, such as pulmonary arterial or venous wall irregularity, eccentric location of thrombi, and focal dilatation or tortuosity of pulmonary arteries with filling defects, were found that could have favoured thrombosis in situ rather than an embolic cause. Although the lack of specific findings does not exclude in situ pulmonary thrombosis, DECT-PA differentiation of in situ thrombosis from PE is limited. The presence of mixed or consolidative opacities adjacent to most pulmonary arterial filling defects (12/25 patients, 80%) could suggest diffuse or advanced pneumonia in these patients or an increased thrombogenic potential of these opacities compared to pure ground-glass opacities.

The qualitative interpretation of MDI for iodine is subject to errors due to variability in scanner type and image reconstruction techniques. The pure ground-glass opacities tend to have a higher qualitative perfusion irrespective of location in both SS-DECT and DS-DECT scanners. The qualitative hyperperfusion in ground-glass opacities on MDI images was likely a perception issue as there was no significant difference in QPS between ground-glass opacities and normal lung parenchyma ($p=0.73$). This perception issue may be related to the fact that the ground-glass opacities have low negative attenuation values (often well below -300 HU). Such low CT number implies that ground-glass opacities will not be excluded from MDI images, and thus, give a visual appearance of increased perfusion without a measurable increase in iodine content. To the authors' best knowledge, the exclusion of ground-glass opacities from processed MDI images has not been reported and underscores the importance of quantitative measurement of values on MDI images, which are typically

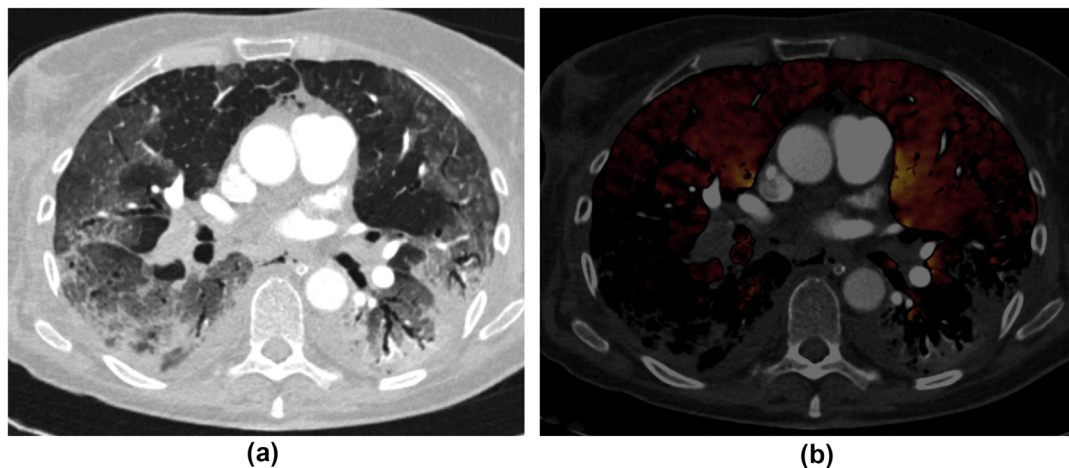


Figure 5 (a) Transverse chest CT image in lung window of a 45-year-old woman with COVID-19 pneumonia demonstrates mixed consolidation and ground glass in the bilateral lower lobes along with multifocal ground-glass opacities in the upper lobes. (b) At the same anatomical level, the transverse MDI image (a fused image of lung perfusion overlaid on conventional CT image in a soft-tissue window) depicts large pulmonary emboli in the right lower lobar and segmental arteries. The decreased perfusion in the right lower lobe is attributed to a perfusion defect from occlusive PE. The lack of perfusion in the left lower lobe without corresponding PE is artefactual as regions with consolidation are excluded from evaluation.

acquired by subtracting water from iodine and will not visualise lesions with attenuation less than that of water (ground-glass opacities). In contrast, whereas consolidative opacities tend to have increased or heterogeneous iodine distribution in SS-DECT-PA and decreased iodine distribution in DS-DECT-PA. These differences were likely related to differences in how the vendors approach dual-energy image or data processing for generating MDI images or based perception of MDI images by the radiologists. The MDI images from DS-DECT-PA datasets identify the air attenuation portions of the lungs and exclude regions with higher attenuation, such as consolidation, which makes the latter appear hypoperfused. Although lung regions with higher attenuation, such as consolidation, can be included in the MDI images by changing the maximum threshold in the image processing software, we did not change the default threshold as it alters the image appearance and makes them less sensitive for detection of true ischaemia-related perfusion defects. Conversely, the MDI images from SS-DECT-PA does not isolate air-attenuation lungs and includes regions of consolidation; the latter could be therefore assessed qualitatively with increased or heterogeneous perfusion on MDI images. Previous studies have also reported differences in appearance of DECT-PA images between different vendors.¹⁹ Therefore, the increased iodine distribution noted in ground glass halo around consolidation in DS-DECT-PA does not necessarily imply “hyperaemic halo”.^{12,13} Similarly, the findings of dilated pulmonary arteries and increased subpleural vessels reported by the same authors were not noted in the present series. Dilated or prominent vessels could be a reflection of decreased lung volumes related to atelectasis or fibrotic process (from an apparent foreshortening of vessels with volume loss which enables tracking of larger vessels to more peripheral lungs) or fibrosis, and it is also difficult to explain the development of subpleural collaterals in a short course of illness.

The present study has several limitations. DECT-PA was performed on three different CT scanners, which may have affected the quantitative evaluation of MDI images as images belonging to a SS-DECT CT scanner could not be processed with QPS software. Another limitation pertains to the lack of representation of patients with DECT-PA without suspected or known PE as most patients without known or clinically suspected PE undergo non-contrast chest CT without dual-energy scan mode. Although most PE detected in the present study were located within the subsegmental arteries (29/53), extensive pulmonary opacities could have limited the detection of additional subsegmental PE and perfusion defects on DECT-PA. This limitation was evident from the fact that regions with ground-glass opacities demonstrated an apparent hyperperfusion and consolidation was associated with a variable change in perfusion based on the DECT vendor. Another limitation of the study pertains to the fact that QPS were assessed over anatomical regions of interest rather than confined to regions with different opacity types. Although subjective assessment of qualitative perfusion was performed in lung regions with and without pulmonary opacities, the QPS only quantifies perfusion in the aerated portion of the lungs

and not in regions with dense opacities regardless of their aetiology (ischaemic or non-ischaemic). The present results on predicting patient outcome from DECT-PA must be interpreted with caution as a control arm of patients without COVID-19 pneumonia was not included and the patients were not distributed symmetrically between different therapies.

In summary, there is a high prevalence of pulmonary arterial filling defects in patients with COVID-19 infection, and QP obtained from DECT-PA provide useful information on the severity of disease and outcomes of COVID-19 pneumonia. Users must understand the limitation of both DECT-PA and QPS in patients with parenchymal opacities related to COVID-19 pneumonia as these opacities confound the evaluation of qualitative and quantitative perfusion changes in lungs.

Conflict of interest

A coauthor (MKK) has received research grants from Siemens Healthineers and Riverain Tech Inc. for separate research. Another coauthor (SRD) has received research grants from Lunit Inc, and GE Healthcare for unrelated projects.

References

- McGonagle D, O'Donnell J, Sharif K, et al. Immune mechanisms of pulmonary intravascular coagulopathy in COVID-19 pneumonia. *Lancet Rheumatol* 2020, [https://doi.org/10.1016/S2665-9913\(20\)30121-1](https://doi.org/10.1016/S2665-9913(20)30121-1).
- Varga S, Flammer A, Steiger P, et al. Endothelial cell infection and endothelitis in COVID-19. *Lancet* May 2020; **10234**:1417–8.
- Lodigiani C, Iapichino G, Carenzo L, et al. Venous and arterial thromboembolic complications in COVID-19 patients admitted to an academic hospital in Milan, Italy. *Thromb Res* 2020; **191**:9–14.
- Mahammed A, Saba L, Vagal A, et al. Imaging in neurological disease of hospitalized COVID-19 patients: an Italian multicenter retrospective observational study. *Radiology* May 2020, <https://doi.org/10.1148/radiol.2020201933>.
- Oxley TJ, Mocco J, Majidi S, et al. Large-vessel stroke as a presenting feature of Covid-19 in the young. *N Engl J Med* 2020; **382**(20):e60.
- Middeldorp S, Coppens M, van Haaps TF, et al. Incidence of venous thromboembolism in hospitalized patients with COVID-19. *J Thromb Haemost* 2020, <https://doi.org/10.1111/jth.14888>.
- Klok FA, Kruip MJHA, van der Meer NJM, et al. Confirmation of the high cumulative incidence of thrombotic complications in critically ill ICU patients with COVID-19: an updated analysis. *Thromb Res* 2020 Jul; **191**:148–50.
- Oudkerk M, Buller H, Kujipers D, et al. Diagnosis, prevention, and treatment of thromboembolic complications in COVID-19: report of the National Institute for Public Health of The Netherlands. *Radiology* Apr 2020; **297**:E216–22. <https://doi.org/10.1148/radiol.2020201629>.
- Deshpande C. Thromboembolic findings in COVID-19 autopsies: pulmonary thrombosis or embolism? *Ann Intern Med* 2020; **173**:394–5. <https://doi.org/10.7326/M20-3255>.
- Weidman EK, Plodkowski AJ, Halpenny DF, et al. Dual-energy CT angiography for detection of pulmonary emboli: incremental benefit of iodine maps. *Radiology* 2018; **289**:546–53.
- Singh R, Nie R, Homayounieh F, et al. Quantitative lobar pulmonary perfusion assessment on dual-energy CT pulmonary angiography: applications in PE. *Eur Radiol* 2020; **30**:2535–42.
- Lang M, Som A, Mendoza D, et al. Hypoxaemia related to COVID-19: vascular and perfusion abnormalities on dual-energy CT. *Lancet Infect Dis* 2020; **20**:1365–6. [https://doi.org/10.1016/S1473-3099\(20\)30367-4](https://doi.org/10.1016/S1473-3099(20)30367-4).

13. Lang M, Som A, Carey D, et al. Pulmonary vascular manifestations of COVID-19 pneumonia. *Radiol Cardiothorac Imag* Jun 2020;**2**(3):e200277. <https://doi.org/10.1148/ryct.2020200277>.
14. Grillet F, Busse-Coté A, Calame P, et al. COVID-19 pneumonia: microvascular disease revealed on pulmonary dual-energy computed tomography angiography. *Quant Imaging Med Surg* 2020 Sep;**10**(9):1852–62.
15. Ridge CA, Desai SR, Jeyin N, et al. Dual-energy CT pulmonary angiography (DECTPA) quantifies vasculopathy in severe COVID-19 pneumonia. *Radiol Cardiothorac Imaging* 2020;**2**(5):e200428. <https://doi.org/10.1148/ryct.2020200428>.
16. Bernheim A, Mei X, Huang M, et al. Chest CT findings in coronavirus disease-19 (COVID-19): relationship to duration of infection. *Radiology* 2020 Jun;**295**(3):200463. <https://doi.org/10.1148/radiol.2020200463>.
17. Pan F, Ye T, Sun P, et al. Time course of lung changes on chest CT during recovery from 2019 novel coronavirus (COVID-19) pneumonia. *Radiology* 2020 Feb 13;**295**:715–21. <https://doi.org/10.1148/radiol.2020200370>.
18. Poissy J, Goutay J, Caplan M, et al. PE in COVID-19 patients: awareness of an increased prevalence. *Circulation* 2020 Apr 24;**142**:184–6. <https://doi.org/10.1161/CIRCULATIONAHA.120.047430>.
19. Singh R, Sharma A, McDermott S, et al. Comparison of image quality and radiation doses between rapid kV-switching and dual-source DECT techniques in the chest. *Eur J Radiol* 2019;**119**:108639.